Spectroscopic Analysis of Lithium Fluoride (LiF) using Laser Ablation

Saifullah Jamali[1], Waseem Ahmed Bhutto[1], Altaf H. Nizamani[1], Hussain Saleem[2*], Murad Ali Khaskheli[1], Abdul Majid Soomro[1], Ali Ghulam Sahito[3], Nek Muhammad Shaikh[1], Samina Saleem[2,4]

[1]Institute of Physics, University of Sindh, Jamshoro, Pakistan.
[2]Department of Computer Science, UBIT, University of Karachi, Karachi, Pakistan.
[3]Centre for Pure & Applied Geology, University of Sindh, Jamshoro, Pakistan.
[4]Karachi University Business School, KUBS, University of Karachi, Pakistan.
**Corresponding Author: hussainsaleem@uok.edu.pk*

Abstract
This paper presents a study of plasma emission from Lithium Fluoride surface produced by Q-switch Laser (Nd: YAG Laser) having 1064 nm wavelength. The sample has been targeted with Q-switch laser pulses at atmospheric pressure in air. Only neutral Lithium (Li) is confirmed in the emission spectrum of Lithium Fluoride plasma. The Boltzmann distribution technique was used to calculate Electron Temperature (T_e) . Similarly, Stark Broadening Profile (SBP) technique was used to calculate the Electron Number Density (N_e) . T_e is estimated at variable distances along the propagation of plasma plume from the sample surface. Beside that we studied the changing of N_e as a function of distance along the propagation of plasma plume from the surface of the sample. We have also calculated the Inverse Bremsstrahlung (IB) absorption co-efficient and its variation along the distance. It is observed that the T_e, N_e and IB absorption co-efficient decreases as distance increases. In addition, self-absorption of radiation also decreases as temperature decreases.

Key words:
Electron number density; Electron temperature; Inverse Bremsstrahlung Co-efficient; Laser Ablation; Lithium Fluoride;

1. Introduction

The production of plasmas of high temperature and high dense by targeting a powerful laser pulse to sample surface is quiet a developing field in engineering, basic sciences as well as in material processing technology (MPT) [1]. Laser induced breakdown spectroscopy (LIBS) is a multipurpose method used for fast chemical analysis and based on the Atomic Emission Spectroscopy (AEM). During this technique, the powerful laser photons irradiated on sample surface. As a result small portion of a sample surface converts into plasma which contains vaporize, ionize and excite species [2][3][4]. On the recombination, plasma cool down and emits light (characteristic radiation) which were accumulated and spectrally investigated for the functional details of spectroscopic analysis just like electron temperature (T_e) as well as number density (N_e) of the plasma.

The plasma formation normal to the sample surface pivot depends on laser properties such as (wavelength, energy, as well as on pulse duration) and sample properties such as (optical properties as well as on thermodynamic properties) [5][6][7]. There are various applications of Lithium Fluoride (LiF). Used as a flux for ceramics production and also used in welding and brazing fluxes. In addition, Lithium Fluoride has vast band gap that have many applications in vacuum ultra-violet optics.

Because of non-hydroscopic, excellent transmission and high radiation destruction threshold, LiF windows or glasses are mainly operated for the photo absorption investigation in vacuum ultra-violet region [8][9]. Lithium (Li) is a key element in the Fluoride form windows. Therefore, detailed study of the construction of Li in such domains opens and produce exciting knowledge.

Labazan and Milosevic [8] estimated the electron number density for laser produced Li plasma plume by utilizing cavity ring down spectroscopy. Vazquez et al. [10] estimated the electron temperature (T_e) as well as electron number density (N_e) for LiF plasma generated through nano-second UV laser ablation. Labazan et al. [11] calculated the laser ablation for Li as well as $LiCd$ alloy by using flight time mass spectroscopy. Boewe et al. [12] has shown the results of deep pumping on spatial as well as temporal development of the Lithium plasma produced by laser photon.

Bailey et al. [13] calculated the time resolved spectra for Lithium plasma generated by dye laser. Cvejis et al. [14] examine the Lithium line vitality whole part in plasma at low temperature. Frolov et al. [15] examines that even low powerful pulse of incident laser is adequate for making of obvious remove plume of plasma over the surface of Lithium Fluoride as well as Caesium iodide (CsI) test samples. Aslam et al. [16] investigated subjectively LiF plasma through laser removal process and they noticed only neutral Lithium spectral lines by a technique known as laser ablation.

In the current work we have utilized LIBS (Laser Induced Breakdown Spectroscopy) method to examine the commercially available LiF window plasma using Q-switch nanosecond Nd: YAG laser in fundamental mode.

Manuscript received August 5, 2019
Manuscript revised August 20, 2019

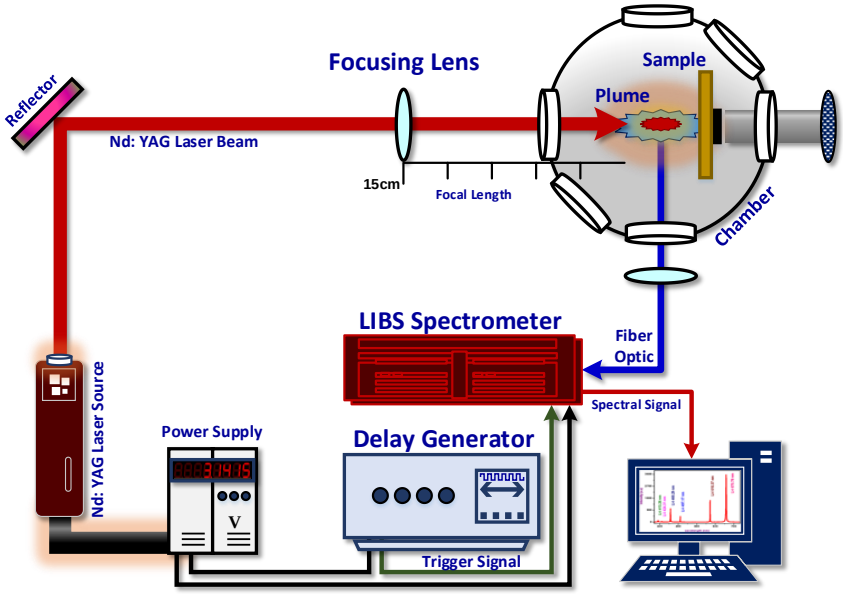

Fig.1. The experimental arrangement of spectroscopic analysis of Lithium Fluoride (LiF) using laser ablation [21].

2. The Experimental Arrangement

The plasma was generated by using Nd: YAG laser in fundamental mode (5 ns pulse width, 10 Hz repetition rate and 400 mJ energy mode). Joule meter (Nova-Quantel P/niz 01507) is used in order to measure the laser energy. The experiment arrangement is adapted from Ref. [21] as shown in Fig.1. Laser beam was striked towards the sample surface via focusing lens having 15 cm focal length. To avoid the unwanted interaction among air molecules and Nd: YAG laser beam, the focal length of the focusing lens is selected in such a way that the laser pulses remain focused only on the surface of the sample. As plasma cools down by emitting characteristic radiation, LIBS 2000+ spectrometer was set to record all the emitted radiations collected through optical fiber which was aligned at 90° degree to the plasma plume and produced spectral lines (spectra). Finally, the collected LIBS emission spectrum was analyzed using the OriginLab® software [32][33][34][35][36].

3. Results and Discussion

3.1 The Atomic Emission Spectrum of Lithium Fluoride Plasma

In the present work, we have examined Lithium Fluoride (LiF) plasma created by Nd: YAG laser operated at fundamental mode by putting the targeted sample (LiF) in air at the atmospheric pressure. Fig.2, exhibits the atomic emission spectrum of plasma of LiF. It was generated at the surface of the targeted sample by operating Q-switched 1064 nm Nd: YAG Laser.

After analyzing the emission spectrum, it was compared through NIST spectral atomic data base while unsheltered the existent of Lithium neutral lines, found that no singly ionized line of Lithium was observed. The structure at:

- 413.26 nm is identified as $5d\ ^2D_{5/2} \rightarrow 2p\ ^2P_{3/2}$,
- 427.31 nm is identified as $5s\ ^2S_{1/2} \rightarrow 2p\ ^2P_{3/2}$,
- 460.29 nm is identified as $4d\ ^2D_{5/2} \rightarrow 2p\ ^2P_{3/2}$,
- 497.17 nm is identified as $4s\ ^2S_{1/2} \rightarrow 2p\ ^2P_{3/2}$,
- 610.37 nm is identified as $3d\ ^2D_{5/2} \rightarrow 2p\ ^2P_{3/2}$ and
- $Li - I$ 670.78 nm is identified $2p\ ^2P_{3/2} \rightarrow 2s\ ^2S_{1/2}$ respectively.

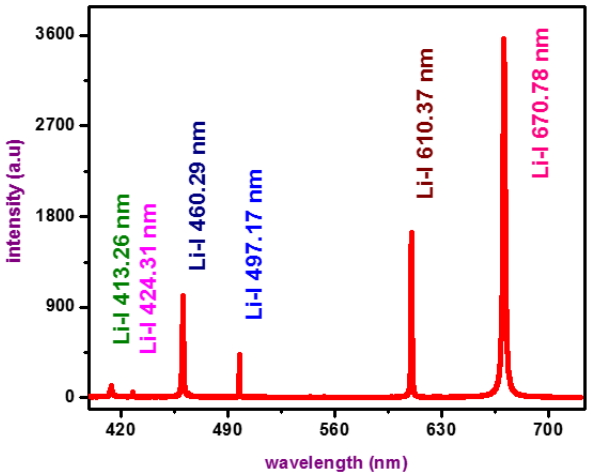

Fig.2. The emission spectrum of Lithium Fluoride (LiF) using Q-switch Nd: YAG laser (1064 nm).

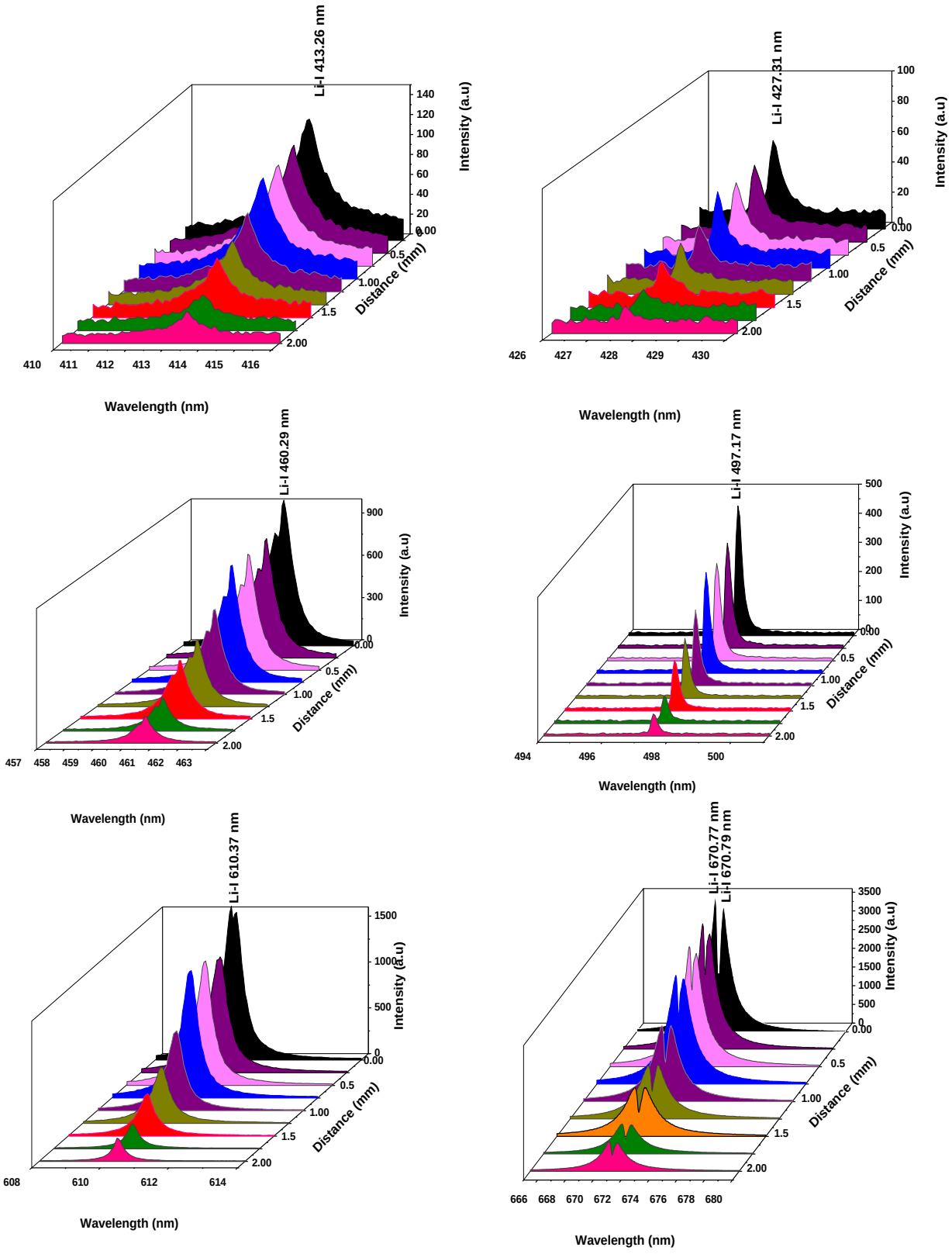

Fig.3. Variation of signal intensity of observed neutral Lithium lines along with distance ($0\sim2\ mm$).

Table.1: Spectroscopic parameters of $Li-I$ lines are used to calculate electron temperature.

Wavelength $\lambda\ (nm)$	Transitions	Statistical Weight		Transition Probability $A_{ki}\ (s^{-1})$	Excitation Energy $E_k\ (cm^{-1})$
		g_k	g_i		
413.26	$5d\ ^2D_{5/2} \rightarrow 2p\ ^2P_{3/2}$	6	4	1.09×10^7	39094.94
427.31	$5s\ ^2S_{1/2} \rightarrow 2p\ ^2P_{3/2}$	2	4	3.17×10^6	38299.50
460.29	$4d\ ^2D_{5/2} \rightarrow 2p\ ^2P_{3/2}$	6	4	2.32×10^7	36623.40
497.17	$4s\ ^2S_{1/2} \rightarrow 2p\ ^2P_{3/2}$	2	4	6.92×10^6	35012.06
610.37	$3d\ ^2D_{5/2} \rightarrow 2p\ ^2P_{3/2}$	6	4	6.85×10^7	31283.12

The plasma's spatial characteristics were inspected by analyzing the emission spectrum of LiF plasma at various distances along the perpendicular path of plasma plume at atmospheric pressure. The intensities of each neutral atomic transition lines of LiF sample has maximum value at 0 mm distance away from the sample surface and intensities of each transition line continuously decreases as the distance increases from 0 mm at the surface to 2 mm above it. The variations in intensities of individual signals obtained from various neutral transitions as a function of distance (distance of focusing lens from the sample) are given in Fig.3.

3.2 The Electron Temperature (T_e)

Investigation of the electron temperature for plasma produced by Q-Switch Nd: YAG laser is an important parameter for analyzing the complex events happening in plasma. The calculation of electron temperature gives the information about excitation as well as ionization processes taking place in plasma. The Boltzmann plot method and Saha equation are used to calculate the electron temperature given that the Local Thermodynamic Equilibrium (LTE) is satisfied [17].

For this work, the Boltzmann plot method was used to calculate electron temperature from relative intensities of observed neutral Li lines of Lithium Fluoride plasma created through Nd: YAG laser, assumed that LTE condition is satisfied. The $Eq.(1)$ shows the Boltzmann Plot Method given below [18]:

$$\ln\left(\frac{\lambda_{ki} I_{ki}}{A_{ki} g_k}\right) = \ln\left(\frac{N}{Z}\right) - \left(\frac{E_k}{K T_e}\right) \qquad \cdots (1)$$

Whereas, λ_{ki} is the signal wavelength, I_{ki} is the integrated signal intensity, A_{ki} is the transition probability, g_k is the statistical weight, N is the upper level population, Z is the partition function, E_k is the excitation energy, K is the constant known as Boltzmann constant and T_e is the electron temperature.

For the calculation of electron temperature, the identified $Li-I$ lines and their spectroscopic variables such as wavelength (λ), transition from higher to lower level, statistical weight $(g_k - g_i)$, transition probability (A_{ki}) and excitation energy (E_k) are given in Table-1. The graph shows straight line between $\ln\left(\frac{\lambda_{ki} I_{ki}}{A_{ki} g_k}\right)$ versus E_k with slope equals to $\left(-\frac{1}{K T_e}\right)$. The maximum estimated value of electron temperature is approximately equal to $10121\ °K$ at 0 mm and decreases to $5205\ °K$ as distance increases to 2 mm from the surface. The decreasing value of electron temperature T_e along the distance is due to the de-excitation and cooling process of plasma. The variation of electron temperature along the distance is shown in Fig.4.

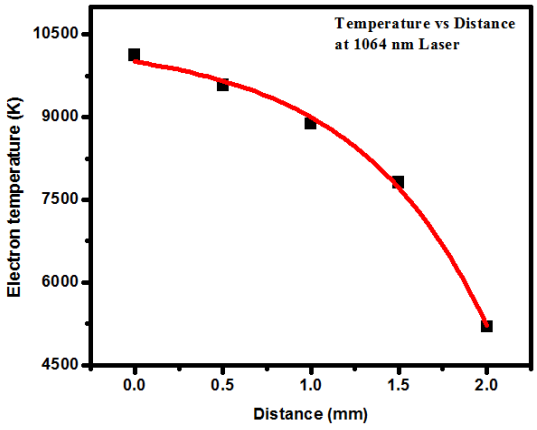

Fig.4. Variation of electron temperature (T_e) along the direction of plasma plume.

3.3 The Electron Number Density (N_e)

In order to calculate plasma variables in Laser Induced plasma, it is compulsory to evaluate the electron number density (N_e). The Starks broadened line profile method was utilized to estimate N_e. For electron number density calculation, following equation is used [19]:

$$\Delta\lambda_{1/2} = 2\omega\left(\frac{N_e}{10^{16}}\right) + 3.5A\left(\frac{N_e}{10^{16}}\right)^{\frac{1}{4}}\left[1 - \frac{3}{4}{N_D}^{-\frac{1}{3}}\right] \times \omega\left(\frac{N_e}{10^{16}}\right) \quad \cdots (2)$$

Whereas, $\Delta\lambda_{1/2}$ is FWHM (Full width at half maximum), ω is electron impact parameter, N_e is electron number density also N_D is the particles number in Debye sphere. $Eq.(2)$ consists of two expressions, the first part evaluates the broadening of electron transition lines and the second part of the expression calculates the broadening of ionic transition lines. The broadening of ionic transition lines is very small and considered as negligible. Thus, for finding the electron number density. $Eq.(3)$ given below is the simplified form of $Eq.(2)$ shown as:

$$\Delta\lambda_{1/2} = 2\omega\left(\frac{N_e}{10^{16}}\right) \quad \cdots (3)$$

To calculate the electron number density in plasma of LiF sample, the neutral Li at $460.29\,nm$ is identified as $4s\,^2D_{5/2} \rightarrow 2p\,^2P_{3/2}$ is used. The FWHM of signal lines is taken out from Lorentzian fit, whereas the impact parameter is accessible in literature [20]. The number density of plasma depends on laser parameters such as laser energy as well as laser wavelength.

The maximum estimated value of electron number density is found to be approximately equal to $1.03 \times 10^{16}\ cm^{-3}$ at $0\,mm$ and its value decreases up to $2\,mm$ distance because of dominancy of plasma recombination, heat conduction and ablation rate. The electron number density varies from $1.03 \times 10^{16}\ cm^{-3}$ to $7.8 \times 10^{14}\ cm^{-3}$ as distance increases from $0\,mm$ to $2\,mm$ as shown in Fig.5.

3.4. The Inverse Bremsstrahlung Co-efficient (α_{IB})

Since the electron temperature as well as electron number density can be utilized to investigate the phenomenon of plasma formation. During laser induced plasma generation, inverse bremsstrahlung (IB) as well as photo ionization (PI) are two major factors of heating of plasma through the radiation. During inverse bremsstrahlung, an electron absorbs a photon in the field of an atom or ion. The IB process is expressed as inverse bremsstrahlung co-efficient (α_{IB}) as given below:

$$\alpha_{IB} = (1.37 \times 10^{-35})\,\lambda^3\,{N_e}^2\,{T_e}^{-1/2} \quad \cdots (4)$$

Where; $\lambda\ (\mu m)$ is photon's wavelength, $N_e\ (cm^{-3})$ is the electron number density and $T_e\ (°K)$ is the electron temperature. It is clear from above $Eq.(4)$ that α_{IB} depends on λ^3. So the inverse bremsstrahlung is more dominant factor for higher wavelength or fundamental mode ($1064\,nm$) and for the shorter wavelengths, the photo ionization is more dominant factor.

The IB co-efficient confirms that the absorption of plasma through inverse bremsstrahlung is dominating for the laser at $1064\,nm$. The co-efficient of IB absorption has maximum value equal to $1.737 \times 10^{-5}\ cm^{-1}$ at $0\,mm$ distance and its value decreases as distance increases up to $2\,mm$. The value of IB absorption co-efficient varies between $1.737 \times 10^{-5}\ cm^{-1}$ to $1.435 \times 10^{-5}\ cm^{-1}$ as distance increases from $0\,mm$ to $2\,mm$.

In present work, the first upper level of Lithium lies $1.85\,eV$, while the ionization potential is $5.39\,eV$. Hence for IR photons ($1.17\,eV$ at $1064\,nm$) the IB operation of the upper levels is dominant factor than PI process.

Fig.6. represents the estimated inverse bremsstrahlung absorption co-efficient in LiF plasma as a function of distance.

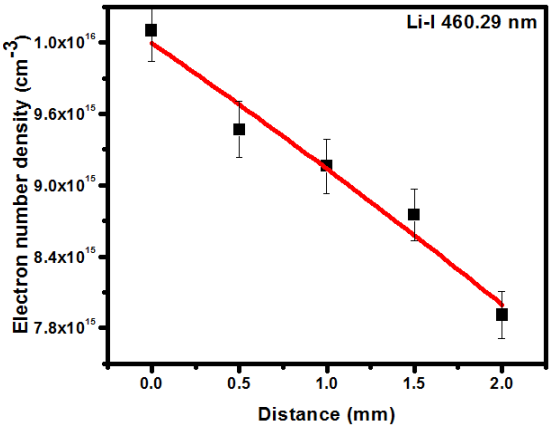

Fig.5. Variation of electron number density (Ne) along with distance ($0{\sim}2\,mm$).

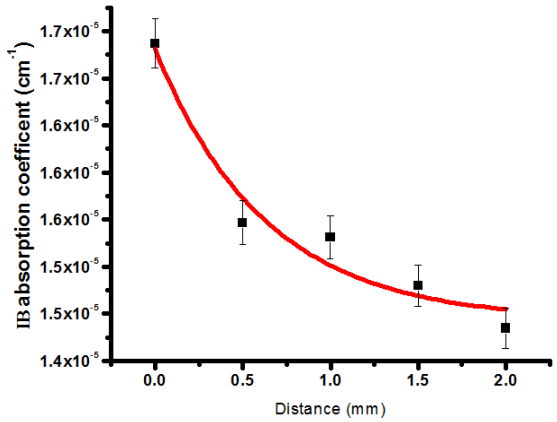

Fig.6. Variation of IB absorption co-efficient along with distance.

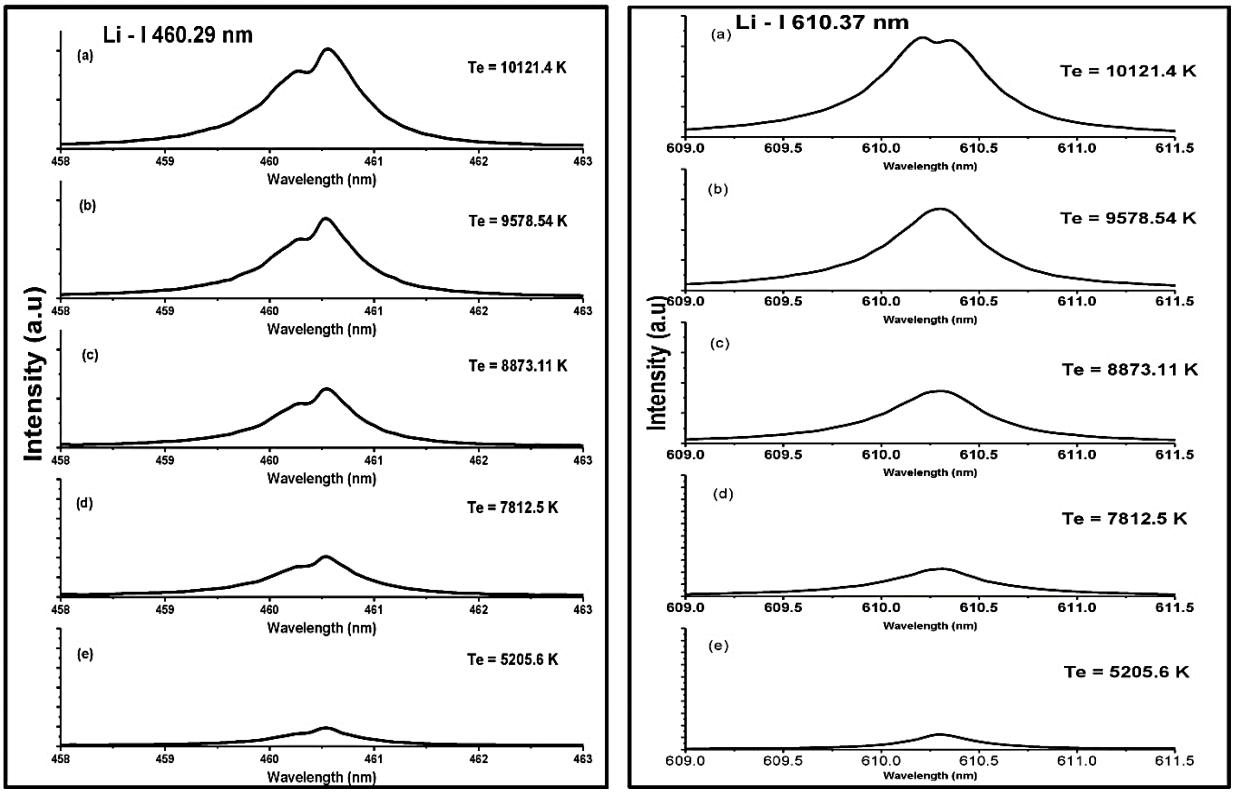

Fig.7. Variation in self-absorption for $Li-I$ 460.29 nm and $Li-I$ 610.37 nm along with distance (0~2 mm).

3.5 Self Absorption

Normally when atoms or ions de-excite they emits photons, so there is a chance that some other atoms of same species absorb the emitted photons given that the photons' energy matches the transition energies of electron in the absorbing atoms or ions. In general, self-absorption are higher for resonance lines of the intrinsic samples. For high density plasma, the plasma plume absorbs its own emission lines.

It is corrected for those transition lines which are connected to the ground state (resonance line) but the other spectral lines may also be affected. The absorption of emitted light is the cause of deformation (dip) in spectral line and the effect is called self-absorption. In LIBS (Laser Induced Breakdown Spectroscopy) experiments, the temperature of plasma decreases towards the outer layer of plasma plume as light passes through the colder layer of plasma plume where the self-absorption occurs significantly.

In case of Lithium Fluoride plasma, we observed self-absorption in two emission lines of neutral Lithium having wavelengths of 460.29 nm and 610.37 nm. In addition, it is observed that as temperature decreases and distance increases, the self-absorption of emission lines continuously decreases as shown in Fig.7. [22][23][24][25][26].

4. Conclusion

We have plotted the relationship between the intensity of neutral lines versus axial distance and observed the maximum intensity at 0 mm distance, as distance increase from 0 mm to 2 mm, the intensity of neutral Lithium lines decreases.

In this work, we have used the Boltzmann Plot Technique for neutral Lithium $Li-I$ spectral lines; 413.26 nm is identified as $5d\ ^2D_{5/2} \rightarrow 2p\ ^2P_{3/2}$, 427.31 nm is identified as $5s\ ^2S_{1/2} \rightarrow 2p\ ^2P_{3/2}$, 460.29 nm is identified as $4d\ ^2D_{5/2} \rightarrow 2p\ ^2P_{3/2}$, 497.17 nm is identified as $4s\ ^2S_{1/2} \rightarrow 2p\ ^2P_{3/2}$, to estimate electron temperature along the axial distance of plasma.

We worked out electron temperature at 0 mm distance to be 10121 $°K$. The electron temperature also decreases as the distance increases from the surface of the target material. In spatial variation, the electron temperature varies as (10121 $°K \sim 5205\ °K$). Furthermore, we have used Stark broadening profile for the $Li-I$ at 460.29 nm transition configuration ($4d\ ^2D_{5/2} \rightarrow 2p\ ^2P_{3/2}$) at 0 mm distance [27][28][29][30][31].

The electron number density has been estimated to be $1.03 \times 10^{16}\, cm^{-3}$. The decreasing trend of electron number density also observed as $1.03 \times 10^{16}\, cm^{-3}$ to $7.8 \times 10^{14}\, cm^{-3}$ as distance increases. Finally, it is concluded that, the electron temperature as well as electron number density decreases as the axial distance increases.

It is also noted that the inverse bremsstrahlung (IB) process is more dominant during laser vapor interaction. And this IB process exponentially decreases as axial distance increase. Similarly, the self-absorption (dip) also decreases as temperature decreases.

References

[1] S. Amoruso, R. Bruzzese, N. Spinelli and R. Velotta, (1991) "Characterization of laser-ablation plasmas", J. Phys. B: At. Mol. Opt. Phys. 32, 131-172.

[2] D. A. Cremers and L. J. Radziemski, (2006) "Hand book of laser induced breakdown spectroscopy", Wiley, Chichester.

[3] D. W. Hahn and N. Omenetto, (2012) "Laser-Induced Breakdown Spectroscopy (LIBS), Part II: Review of Instrumental and Methodological Approaches to Material Analysis and Applications to Different Fields", Appl Spectrosc 66, 347–419.

[4] J. P. Singh and S. N. Thakur, (2007) "Laser-induced breakdown spectroscopy", Elsevier, Amsterdam.

[5] M. B. S. Andersen, J. Frydenvan, P. Henckel and A. Rinnan, (2016) "The potential of laser-induced breakdown spectroscopy for industrial at-line monitoring of calcium content in comminuted poultry meat", Food Control 64, 226 - 233.

[6] J. Fortes, D. Maria, P. Carceles, A. Luna and J. Laserna, (2006)" International journal Legal Media" DOI 10.1007/s00414-041-1131-9.

[7] B. Dolgin, Y. Chen and I. Schechter, (2006) "Use of IIBS for rapid characterization of parchment. Anal. Bioanal", Chem. 386, 1535-1541.

[8] X. Y. Liu and W. J. Zhang, (2008) "Recent developments in biomedicine fields for laser induced breakdown spectroscopy", J Biomed Sci Eng 1, 147–151.

[9] I. Labazan, S. Milošević, (2002) "Observation of lithium dimers in laser produced plume by cavity ring-down spectroscopy", Chem. Phys. Lett. 352, 226–233.

[10] F. J. Gordillo-Vazquez, A. Perea, A. P. McKiernan, and C. N. Afonso, (2005) "Electronic temperature and density of the plasma produced by nanosecond ultraviolet laser ablation of LiF", Appl. Phys. Lett.86, 181501.

[11] I. Labazan, E. Vrbanek, S. Milosevic, and R. Duren, (2005) "Laser ablation of lithium and lithium/cadmium alloy studied by time-of-flight mass spectroscopy", Appl. Phys. A80, 569–574.

[12] P. Boewe, J. Conway, P. Dunne, T. M. Cormack, and G. O'Sullivan, (1999) "Effects of resonant pumping on the temporal and spatial evolution of a laser produced lithium plasma", J. Appl. Phys.86, 3002.

[13] J. Bailey, G. C. Tisone, M. J. Hurst, R. L. Morrison, and K. W. Beig, (1988) "Time-resolved visible spectroscopy of laser-produced lithium plasmas", Rev. Sci. Instrum.59, 1485.

[14] M. Cvejic, E. Stambulchik, M. R. Gavrilovic, S. Jovicevic and N. Konjevic, (2014) "Neutral lithium spectral line 460.28 nm with forbidden component for low temperature plasma diagnostic of laser-induced plasma", 86-97.

[15] O. Frolov, K. Kolacek, J. Schmidt, J. Straus, A. Choukourov and P. Pira, (2016) "Ablation of LiF and CsI By EUV Nanosecond Laser Pulse", 98.

[16] M. A. Baig, A. Qamar, M. A. Fareed, M. Anwar-ul-Haq and R. Ali, (2012) "Spatial Diagnostics of the laser induced lithium fluoride plasma". Phys. Of plasmas 19, 063304.

[17] J. A. Aguilera and C. Aragon, (2004) "Characterization of a laser-induced plasma by spatially resolved spectroscopy of neutral atom and ion emission", Spectrochim. Acta, Part B59, 1861-1876.

[18] I. Rehan, K. Rehan, S. Sultana, M. Our-ul-Haq, M. Z. khan Niazi and R. Muhammad, (2016) "Spatial characterization of red and white skin potatoes using nano-second induced breakdown in air", Eur. Phys. J. Appl. Phys. 73, 10701.

[19] A. W. Miziolek, V. Palleschi, I. Schechter, (2006) "Laser Induce Breakdown Spectroscopy" (Cambridge University Press).

[20] N. Konjevic and J. R. Roberts, (1976) "A Critical Review of the Stark widths and Shifts of Spectral Lines from No-Hydrogenic Atoms", J. Phys. Chem. Ref. Data, 5, 2.

[21] N. M. Shaikh, S. Hafeez, B. Rashid, S. Mahmood and M. A. Baig, (2006), "Optical emission studies of the mercury plasma generated by the fundamental, second and third harmonics of a Nd : YAG laser", J. Phys. D: Appl. Phys. 39, 4377–4385.

[22] M. Y. Channa, A. H. Nizamani, H. Saleem, W. A. Bhutto, A. M. Soomro, and M. Y. Soomro, (2019), "Surface Ion Trap Designs for Vertical Ion Shuttling," IJCSNS International Journal of Computer Science and Network Security, vol. 19, no. 4.

[23] H. Saleem, A. H. Nizamani, W. A. Bhutto, A. M. Soomro, M. Y. Soomro, A. Toufik, (2019), "Two Dimensional Natural Convection Heat Losses from Square Solar Cavity Receiver," IJCSNS International Journal of Computer Science and Network Security, vol. 19, no. 4.

[24] A. M. Soomro, W. A. Bhutto, A. H. Nizamani, H. Saleem, M. Y. Soomro, M. A. Khaskheli, N. M. Shaikh, (2019), "Controllable Growth of Hexagonal BN Monolayer Sheets on Cu Foil by LPCVD," IJCSNS International Journal of Computer Science and Network Security, vol. 19, no. 6.

[25] R. Chand, Saeeduddin, M. A. Khaskheli, A. M. Soomro, H. Saleem, W. A. Bhutto, A. H. Nizamani, M.Y. Soomro, N. M. Shaikh, S. V. Muniandy, (2019), "Fractal Analysis of Light Scattering Data from Gravity-Driven Granular Flows," IJCSNS International Journal of Computer Science and Network Security, vol. 19, no. 7.

[26] M. Y. Channa, A. H. Nizamani, A. M. Soomro, H. Saleem, W. A. Bhutto, M. Y. Soomro, M. A. Khaskheli, N. M. Shaikh, (2019), "Vertical Ion Shuttling Protocols for Multi-Strip Surface Ion Traps," IJCSNS International Journal of Computer Science and Network Security, vol. 19, no. 7.

[27] W. A. Bhutto, A. M. Soomro, A. H. Nizamani, H. Saleem, M. A. Khaskheli, A. G. Sahito, R. Das, U. A. Khan, S. Saleem, (2019), "Controlled Growth of Zinc Oxide Nanowire Arrays by Chemical Vapor Deposition (CVD) Method," IJCSNS International Journal of Computer Science and Network Security, vol. 19, no. 8.

[28] A. H. Nizamani, B. Rasool, M. Tahir, N. M. Shaikh, H. Saleem, (2013). "Adiabatic ION Shuttling Protocols in Outer-Segmented-Electrode Surface ION Traps," International Journal of Scientific & Engineering Research (IJSER), 4(6), 3055-3061.

[29] A. H. Nizamani, S. A. Buzdar, B. Rasool, N. M. Shaikh, H. Saleem, (2013). Computer-based frequency drift control of multiple LASERs in real-time. International Journal of Scientific & Engineering Research (IJSER), 4(6), 3038.

[30] A. H. Nizamani, M. A. Rind, N. M. Shaikh, A. H. Moghal, H. Saleem, (2013). Versatile Ultra High Vacuum System for ION Trap Experiments: Design and Implementation. Intl. Journal of Advancements in Research & Technology, USA, 2(5).

[31] S. A. Buzdar, M. A. Khan, A. Nazir, M. A. Gadhi, A. H. Nizamani, H. Saleem, (2013). Effect of Change in Orientation of Enhanced Dynamic Wedges on Radiotherapy Treatment Dose. IJoART, 2, 496-500.

[32] H. Saleem & et al., (2019), "Imposing Software Traceability and Configuration Management for Change Tolerance in Software Production," IJCSNS International Journal of Computer Science and Network Security, vol. 19, no. 1.

[33] H. Saleem & et al., (2019), "Novel Intelligent Electronic Booking Framework for E-Business with Distributed Computing and Data Mining," IJCSNS International Journal of Computer Science and Network Security, vol. 19, no. 4.

[34] H. Saleem & et al., (2019), "Data Science and Machine Learning Approach to Improve E-Commerce Sales Performance on Social Web," IJCSNS International Journal of Computer Science and Network Security, vol. 19, no. 9.

[35] H. Saleem & et al., (2019), "Behavioral Tendency Analysis towards E-Participation for Voting in Political Elections using Social Web," IJCSNS International Journal of Computer Science and Network Security, vol. 19, no. 9.

[36] H. Saleem & et al., (2012), "Review of Various Aspects of Radio Frequency IDentification (RFID) Technology," International Organization for Scientific Research - Journal of Computer Engineering (IOSR-JCE), vol. 8, no. 1.